AGU PUBLICATIONS

JGR

Journal of Geophysical Research: Atmospheres

RESEARCH ARTICLE

10.1002/2015JD024626

Key Points:
- A specific humidity-adjusted Lagrangian diagnostic is applied to arid central Asia
- The northern and southern basins of the Tianshan Mountains show different moisture regimes
- Terrestrial moisture from Europe and central Asia is more dominant than Atlantic moisture

Supporting Information:
- Supporting Information S1

Correspondence to:
M. Zhang and S. Wang,
mjzhang2004@163.com;
geowang@126.com

Citation:
Wang, S., M. Zhang, J. Crawford, C. E. Hughes, M. Du, and X. Liu (2017), The effect of moisture source and synoptic conditions on precipitation isotopes in arid central Asia, *J. Geophys. Res. Atmos.*, *122*, 2667–2682, doi:10.1002/2015JD024626.

Received 8 DEC 2015
Accepted 19 FEB 2017
Accepted article online 22 FEB 2017
Published online 7 MAR 2017

The effect of moisture source and synoptic conditions on precipitation isotopes in arid central Asia

Shengjie Wang[1], Mingjun Zhang[1], Jagoda Crawford[2], Catherine E. Hughes[2], Mingxia Du[1], and Xuemei Liu[1]

[1]College of Geography and Environmental Science, Northwest Normal University, Lanzhou, China, [2]Australian Nuclear Science and Technology Organisation, Kirrawee DC, New South Wales, Australia

Abstract The stable isotope composition of precipitation has been widely applied to trace moisture sources. In the westerly dominated areas of central Asia, the isotopic composition of precipitation significantly correlates with surface air temperature, and the temperature effect is widely accepted. However, the significance of isotopes in tracing water vapor source is not clear for this region, and a further investigation using event-based observations is still needed. Based on a network around the Tianshan Mountains, the westerly regime of precipitation isotopes is investigated. Although the seasonality of precipitation isotopes for the northern and southern basins of the Tianshan Mountains is similar, the more arid climate and leeward landform of the southern basin lead to weak moisture transport and relatively enriched oxygen isotopes. Of the synoptic systems resulting in heavy precipitation, the central Asian vortex more commonly leads to depleted isotopic ratios in precipitation, which is related to the contribution of northerly moisture and/or surface moisture. The specific humidity-adjusted Lagrangian diagnostic indicates that the heavy precipitation on the southern basin stations usually has relatively local moisture sources in this arid climate and that terrestrial moisture evaporated from Europe and central Asia, rather than marine moisture from the Atlantic Ocean, is more likely to be the direct moisture source. A sensitivity analysis for target height and adjusting threshold of specific humidity is also applied to the improved Lagrangian diagnostic. Overall, the findings were unaffected by different conditions, and the moisture was more likely to be locally sourced, as indicated by higher specific humidity thresholds.

1. Introduction

Water vapor is a highly variable constituent in the atmosphere and plays an important role in global climate change [*Lavers et al.*, 2015; *Ye et al.*, 2015]. The source and long-range transport of water vapor on global and regional scales are vital in the studies of water budget and weather processes [e.g., *Bosilovich and Schubert*, 2002; *Gimeno et al.*, 2013; *Good et al.*, 2015]. Among the methods to identify source-sink relationships of water vapor in the atmosphere, physical water vapor tracers have been widely used in the past decades [e.g., *Gat and Carmi*, 1970; *Salati et al.*, 1979; *Levin et al.*, 2009; *Jouzel et al.*, 2013; *Yao et al.*, 2013; *Good et al.*, 2014; *Li et al.*, 2015, 2016b], with stable isotopes of hydrogen (^{2}H or D) and oxygen (^{18}O) considered as ideal measurable tracers in precipitation and water vapor. Because of the isotopic fractionation that occurs during water phase change in the hydrological cycle, the variations in the stable isotope signatures of vapor and precipitation at synoptic, seasonal, or interannual scales can be modeled to trace moisture sources and describe water vapor transport [*Gimeno et al.*, 2012]. In addition, synoptic conditions influence atmospheric processes and moisture transport and then impact on the precipitation isotopes. Previous studies indicated that high- or low-pressure systems may cause isotopically enriched or depleted precipitation, respectively, because synoptic conditions influence the meteorological variables of vapor condensation as well as the contribution of locally recycled moisture to precipitating vapor [e.g., *Crawford et al.*, 2013; *Guan et al.*, 2013; *Bailey et al.*, 2015; *Steen-Larsen et al.*, 2015].

The Tianshan Mountains (also known as Tien Shan) is one of the main mountain ranges in central Asia spanning more than 30° in longitude and 5° in latitude, forming a relatively wet island in an arid region [*Hu*, 2004; *Sorg et al.*, 2012]. As an important natural resource in an arid and semiarid climate, precipitation and vapor sources around the Tianshan Mountains have attracted great attention in hydrological and climate studies. During the past decades, monthly [e.g., *Zhang and Wang*, 2016; *Liu et al.*, 2009, 2014], daily, or event-based [e.g., *Yao et al.*, 1999; *Pang et al.*, 2011] sampling for precipitation isotopes was discontinuously undertaken

at the Urumqi city and neighboring areas. Based on these isotopic data, previous moisture source tracing using the isotope-based approach has found that the water vapor over the Tianshan Mountains is mainly replenished by the westerlies, rather than the Indian or eastern Asian monsoons [e.g., *Tian et al*., 2007; *Liu et al*., 2009; *Yao et al*., 2013; *Feng et al*., 2013].

These qualitative studies have been based on the seasonal variation of stable oxygen isotopic ratio and deuterium excess (D-excess = δ^2H − 8δ^{18}O) and have also been supported by back trajectories and other meteorological diagnostics. The traditional Lagrangian approach (i.e., using the back trajectory) has been used to verify the relationship between isotope composition and moisture source [e.g., *Feng et al*., 2013], although the potential uncertainty of the air mass trajectory may originate from many aspects including the default tracing duration and target height. Especially, the selection of the backward duration greatly influences the trajectories, and longer duration usually corresponds to a more distant moisture source being considered in addition to more local sources. Some studies have tried to adjust the backward duration time using meteorological parameters like specific humidity along the back trajectory [e.g., *Sodemann et al*., 2008; *Crawford et al*., 2013], but there is no case study in such an arid climate. In addition, using the Global Network of Isotopes in Precipitation database, *Liu et al*. [2015] found that the northwestern and southwestern winds may deliver moisture with different isotopic ratios to this region via westerlies, indicating that the isotopic composition of precipitation around the Tianshan Mountains may contain more information helpful in tracing moisture sources.

It is clear that the previous precipitation isotope sampling sites were located within a small area and, therefore, cannot well describe the varying characteristics of the entire Tianshan Mountains. More importantly, due to the absence of an intensive observation network, detailed isotopic information about moisture transport has not been available in this westerly dominant region. In 2012, a 23-station network for the measurement of stable isotopes in precipitation was established around the Tianshan Mountains in central Asia [*Wang et al*., 2016a]. Recently, the regime of below-cloud evaporation [*Wang et al*., 2016c] and moisture recycling [*Wang et al*., 2016b] in arid central Asia was assessed based on this event-based database. This network provides a good platform to detect the impact of moisture source variation on stable isotopes in precipitation. The objective of this study is to examine (a) the effect of moisture source and synoptic conditions on precipitation isotopes in central Asia based on the observation network and (b) the usability of a specific humidity-adjusted Lagrangian diagnostic under an arid and semiarid setting. The results of this investigation will provide useful information to understand the hydrological processes in central Asia, which is also helpful for other areas with an arid and semiarid climate.

2. Data and Method

2.1. Study Area

The Tianshan Mountains is the main east-west mountain range in central Asia (Figure 1a). The air regime over the Tianshan Mountains is mainly controlled by westerlies all year round, and the long distance from the surrounding oceans leads to very limited precipitation in this region. The Tibetan Plateau, with mean elevation of approximately 4000 m above sea level (asl), hinders most marine moisture from the Indian Ocean and Pacific Ocean, and the scarce precipitation that does occur is usually considered to have originated from the remote Atlantic Ocean. For the Chinese portion of the Tianshan Mountains, the annual mean precipitation at the mountainous area is 409 mm, but the mean precipitation amounts at the north and south basins are 277 mm and 66 mm, respectively [*Shi et al*., 2008]. Vast sand deserts are distributed around the Tianshan Mountains, including the Taklimakan desert (the world's second largest shifting sand desert) to the south. As shown in Figures 1b and 1c, the precipitation mainly occurs in the summer months from April to October, and the precipitation amount in winter months is very low.

2.2. Sample Collection and Isotopic Analysis

In this study, a recently compiled database of stable isotopes in precipitation across the Tianshan Mountains [*Wang et al*., 2016a] was applied to investigate the effect of moisture source. As stated in *Wang et al*. [2016a], a total of 1052 event-based precipitation samples were collected by full-time meteorological observers at 23 meteorological stations from August 2012 to September 2013 (Figure 1). Relative to the mountain range, there are 7, 6, and 10 sampling stations located at the northern slope (abbreviated from N1 to N7), the

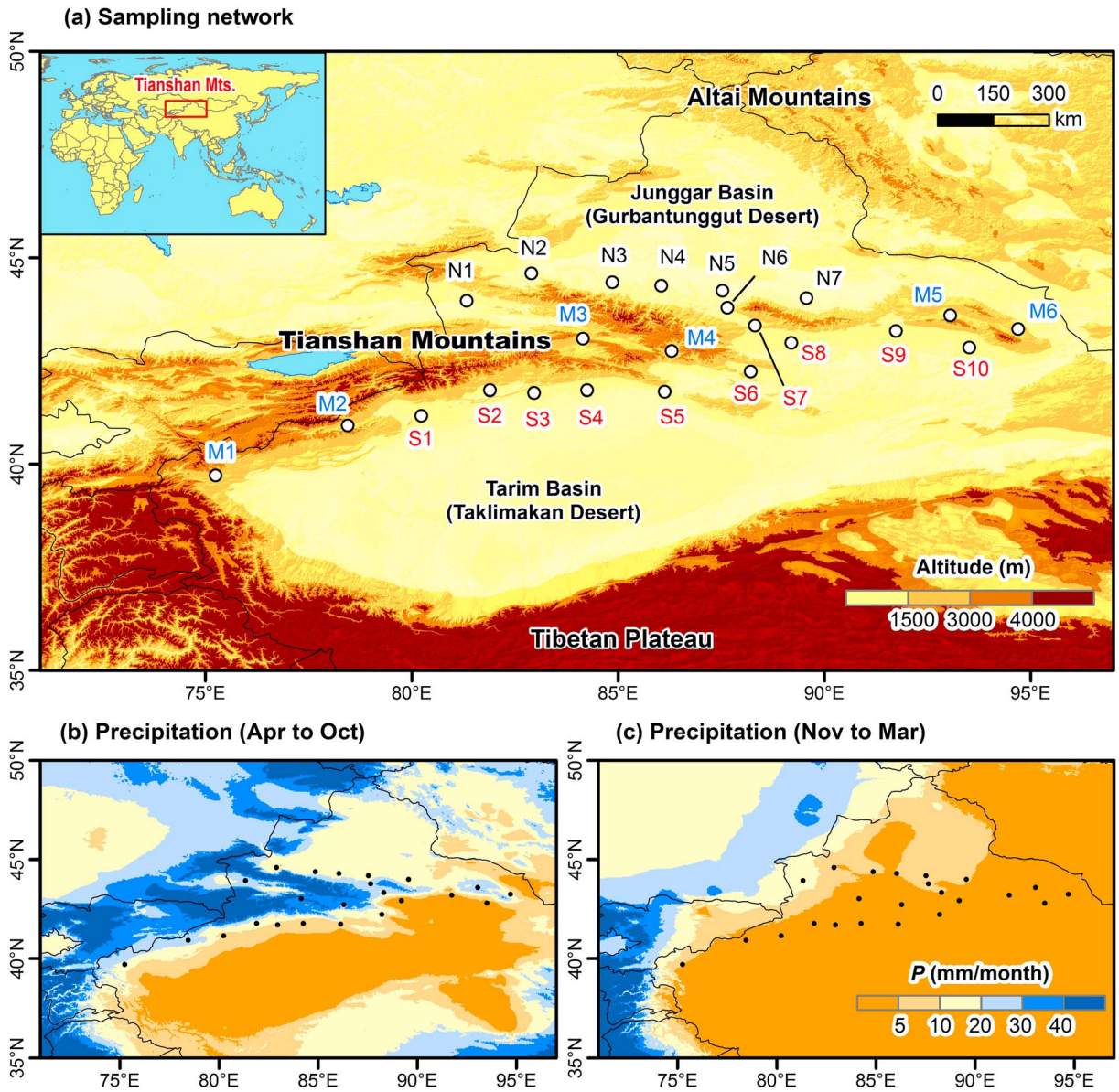

Figure 1. (a) Map showing the locations of sampling sites (empty circles) around the Tianshan Mountains, arid central Asia. The sampling sites are labeled as northern slope: Yining (N1), Jinghe (N2), Kuytun (N3), Shihezi (N4), Caijiahu (N5), Urumqi (N6), and Qitai (N7); mountains: Wuqia (M1), Akqi (M2), Bayanbulak (M3), Balguntay (M4), Barkol (M5), and Yiwu (M6); and southern slope: Aksu (S1), Baicheng (S2), Kuqa (S3), Luntai (S4), Korla (S5), Kumux (S6), Dabancheng (S7), Turpan (S8), Shisanjianfang (S9), and Hami (S10). (b and c) Spatial distributions of monthly mean precipitation in summer months (April–October) and winter months (November–March) during 1950–2000. The long-term climatology is acquired from the WorldClim-Global Climate Data version 1.4 [*Hijmans et al.*, 2005].

mountains (from M1 to M6), and the southern slope (from S1 to S10), respectively. To prevent water evaporation, the liquid samples (rain) were collected immediately after the rainfall ceased and then placed into 60 mL HDPE (high-density polyethylene) bottles with waterproof seals; the solid samples (snow and hail) were collected and then melted in ziplock LDPE (low-density polyethylene) bags at room temperature before being sealed into HDPE bottles. All samples were frozen for storage then fully melted at room temperature prior to analysis. Corresponding meteorological parameters were also measured such as surface air temperature, precipitation amount, and relative humidity during precipitation events. In the 1052 events, there were 813 liquid and 208 solid samples, and the remaining 31 samples were labeled as a mixture (usually sleet). The proportions of precipitation events with amounts <10 mm, <5 mm, and <1 mm were 91.6%, 78.7%, and 35.6%, respectively (Figure 2). The northern slope usually had more

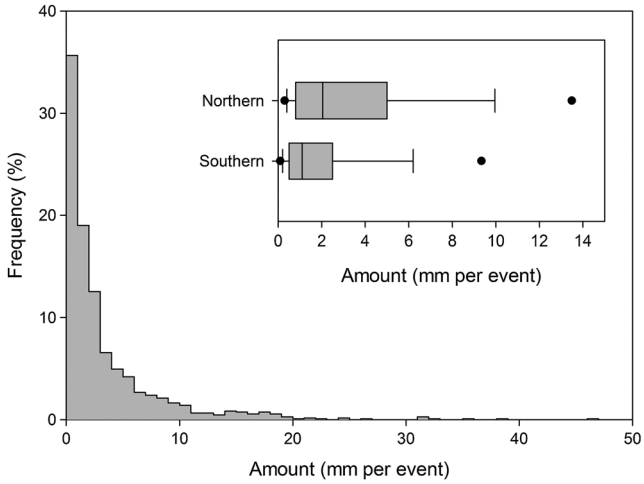

Figure 2. Proportional frequency of precipitation amount per event for all the samples collected at the Tianshan Mountains from August 2012 to September 2013. The small box plot also shows precipitation amount for sampling stations at the northern and southern slopes of the Tianshan Mountains. Boxes represent 25th–75th percentiles, and the line through the box represents the median; whiskers indicate the 90th and 10th percentiles; points above and below the whiskers indicate the 95th and 5th percentiles.

frequent and intense precipitation than the southern slope. The precipitation amounts per event for the northern and southern slope stations were 3.8 ± 4.5 mm and 2.5 ± 4.4 mm, respectively.

The precipitation samples were analyzed using a liquid water isotope analyzer DLT-100 (Los Gatos Research, Inc.) at the Stable Isotope Laboratory, College of Geography and Environmental Science, Northwest Normal University. Every isotopic standard and sample was injected sequentially six times using a microliter syringe, and the arithmetic average of last four injections was accepted as the final result. The measured values are expressed as δ values relative to V-SMOW (Vienna standard mean ocean water):

$$\delta_{\text{sample}} = \frac{R_{\text{sample}} - R_{\text{standard}}}{R_{\text{standard}}} \times 1000‰, \quad (1)$$

where R_{sample} is the ratio of $^2H/^1H$ or $^{18}O/^{16}O$ in the samples and R_{standard} is the ratio of $^2H/^1H$ (0.00015576) or $^{18}O/^{16}O$ (0.0020052) in V-SMOW. The precision is ±0.6‰ for δ^2H and ±0.2‰ for $\delta^{18}O$. More details about sampling and laboratory analyzing were described by *Wang et al*. [2016a].

2.3. Classification of Synoptic Systems

The synoptic systems producing heavy precipitation events (≥10 mm for rain or ≥5 mm for snow) in the study region were systemically summarized by *Zhang and Deng* [1987] and *Zhang and Zhang* [2006] and can be classified into four major types: central Asian vortex (V), central Asian short-wave trough (ST), northern frontal zone trough (NT), and central Asian long-wave trough (LT). Example maps of wind and geopotential height at 500 hPa under these synoptic types are shown in Figure 3. To identify the weather systems resulting in precipitation for the study region, the National Centers for Environmental Prediction/National Center for Atmospheric Research (NCEP/NCAR) Reanalysis 1 [*Kalnay et al*., 1996; *Kistler et al*., 2001] at spatial resolutions of 2.5° (latitude) × 2.5° (longitude) was applied. The NCEP/NCAR Reanalysis 1 database was used to analyze the geopotential height, wind, and vapor flux fields around the Tianshan Mountains. The monthly data were used in calculating geopotential height and wind field at 500 hPa (~5500 m asl) and 700 hPa (~3000 m asl), and the daily data were used in producing water vapor flux field from the surface to 300 hPa and 700 hPa.

2.4. Backward Trajectory Adjusted Using Specific Humidity

To identify the movement of air parcels, a Hybrid Single-Particle Lagrangian Integrated Trajectory (HYSPLIT) model [*Draxler and Hess*, 1998; *Draxler and Rolph*, 2016] version 4 was applied in this study. The HYSPLIT model was developed by the Air Resources Laboratory, National Oceanic and Atmospheric Administration, and has been widely applied in moisture tracing in the past decade [e.g., *Bershaw et al*., 2012; *Crawford et al*., 2013; *Bailey et al*., 2015; *Salamalikis et al*., 2015]. In this study, a HYSPLIT-compatible meteorological data set of Global Data Assimilation System (GDAS) [*Kleist et al*., 2009] with spatial resolution of 1° × 1° was also used.

Using a Lagrangian model, the variation of specific humidity along a backward trajectory can be checked to assess the evaporation and precipitation process [e.g., *Sodemann et al*., 2008; *Crawford et al*., 2013, 2017]. Specifically, the backward trajectories from the sampling sites for each precipitation event were calculated using the HYSPLIT model. The mean residence time of water vapor in the stratosphere is approximately 10 days [*Gat*, 2000; *Trenberth*, 1998], so the backward duration was set as 10 days. In the GDAS data files, related meteorological information is available at a 6 h time resolution, from which specific humidity can be calculated (which we focus on here). For each 6 h interval, if the specific humidity for the following time

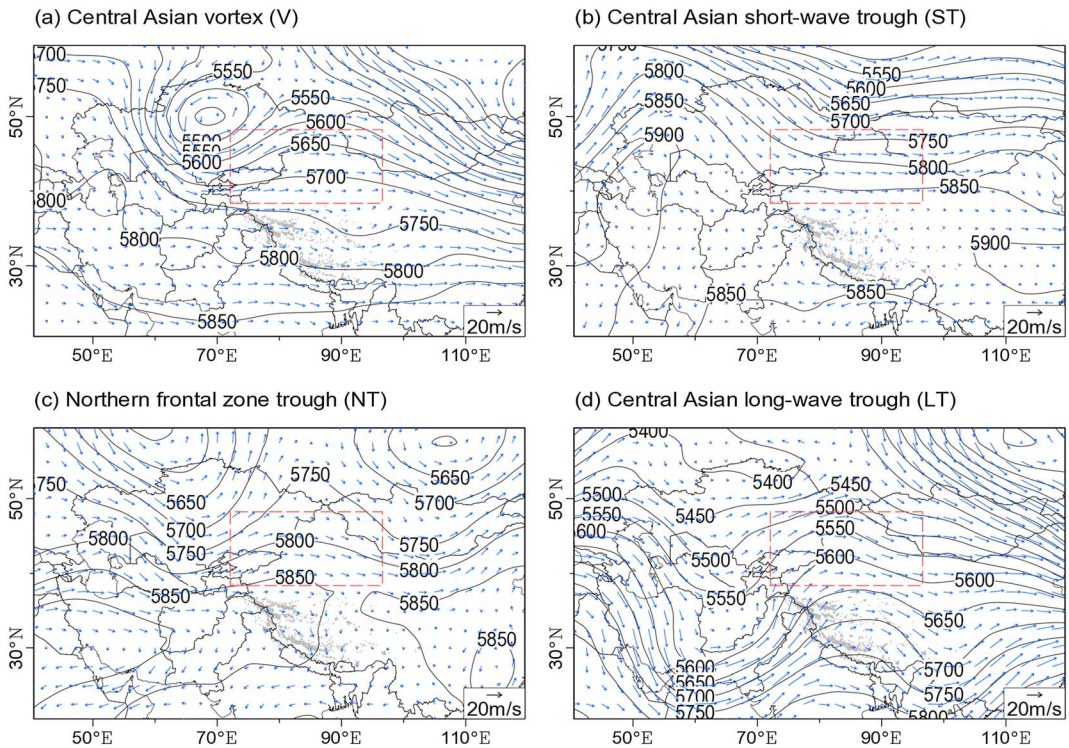

Figure 3. Geopotential height in gpm (geopotential meter) and wind in m/s at 500 hPa for typical synoptic systems influencing precipitation around the Tianshan Mountains: (a) central Asian vortex (V), 20:00 Beijing Time, 17 October 2012; (b) central Asian short-wave trough (ST), 20:00 Beijing Time, 15 August 2012; (c) northern frontal zone trough (NT), 20:00 Beijing Time, 14 July 2013; and (d) central Asian long-wave trough (LT), 8:00 Beijing Time, 4 February 2013. Gray shading indicates elevation >5500 m asl (corresponds to ~500 hPa). Red dashed frames mark the study region.

interval is 0.2 g/kg higher than at the previous time interval, and the modeled height of the air mass is below the planternary boundary layer height, the location of air parcel at the previous time is identified as an evaporative source location [*Sodemann et al*., 2008]. If specific humidity along the trajectory is ≤0.05 g/kg, no more backward tracing is needed. Similar approaches have been applied in Greenland [*Sodemann et al*., 2008] and Australia [*Crawford et al*., 2013, 2017].

In HYSPLIT, the start date/time and location/height for each precipitation event are needed. Four starting heights were applied to the model, i.e., 100 m, 500 m, 1000 m, and 1500 m, above ground level. In addition to 0.2 g/kg, three more threshold values of specific humidity to cut off the trajectories were also tested, i.e., 0.1 g/kg, 0.3 g/kg, and 0.4 g/kg.

3. Results and Discussions

3.1. Precipitation Isotope Seasonality and the Westerly Regime

As stated in *Wang et al*. [2016a], the precipitation stable isotopes in summer months are much more enriched than in winter months across the Tianshan Mountains (Figure 4). Long-term observations of isotopes in precipitation across westerlies-dominated zones of the northern portion of Tibetan Plateau show that δ^{18}O is enriched in summer and depleted in winter [*Tian et al*., 2007; *Yao et al*., 2013]. This is similar to the isotopic signature at the Tianshan Mountains (Figure 4) which suggests that it is dominated by westerlies all year round. In contrast, δ^{18}O in the monsoon domain (southern portion of Tibetan Plateau) [*Yao et al*., 2013] experiences an abrupt decrease in May with greatest depletion in August. However, for many months the westerly and monsoonal signatures are similar; therefore, further investigation of moisture sources is warranted. In addition, the northern and southern slopes show spatial differences in isotopic ratios of precipitation. In summer, with relatively frequent precipitation events, the southern stations are usually more enriched in heavy isotopes, which can be directly seen from the upper whiskers (upper 10th percentiles) and outlier points (upper 5th percentiles) of the box plots in Figure 4.

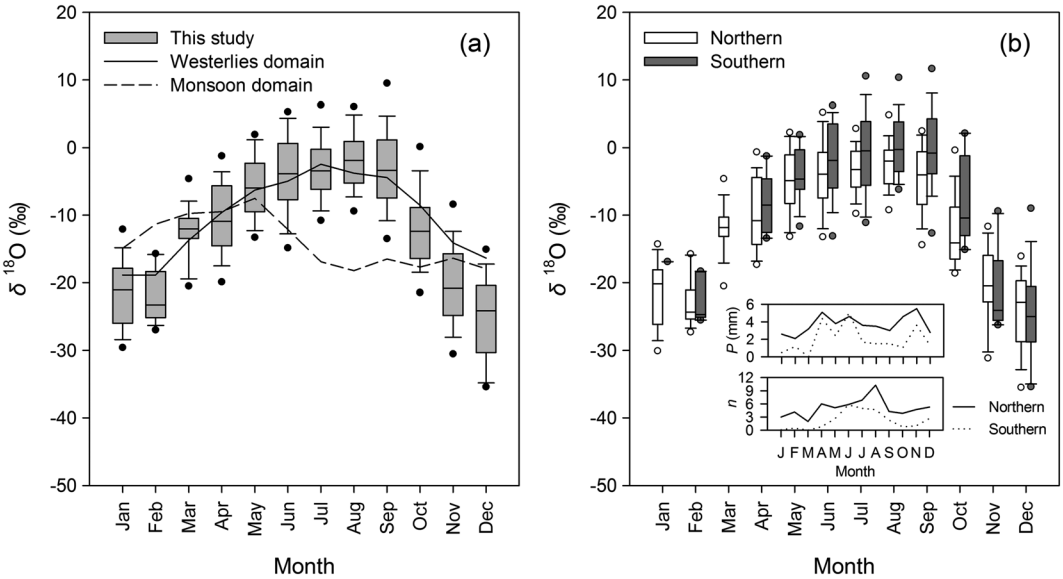

Figure 4. Monthly variation of δ^{18}O in precipitation at (a) all sampling sites and (b) northern and southern slopes of the Tianshan Mountains from August 2012 to September 2013. Boxes represent 25th–75th percentiles, and the line through the box represents the median; whiskers indicate the 90th and 10th percentiles; points above and below the whiskers indicate the 95th and 5th percentiles. The monthly variation of δ^{18}O in observed precipitation for the westerlies and monsoon domain in High Asia [*Yao et al.*, 2013] is shown in Figure 4a. Precipitation amount per event (*P*) and sample number per station (*n*) for northern and southern slopes are shown in the insets of Figure 4b.

Reanalysis database-derived moisture fluxes can be used to verify the westerly regime influencing the seasonality of isotopes in precipitation of the study region. At the air pressure of 500 hPa (Figures 5a and 5b), the geopotential height contours in the study region are generally parallel with latitude, and the wind speeds for the northern and southern slopes of the Tianshan Mountains are similar. In contrast, at 700 hPa (Figures 5c and 5d), the wind fields for the two sides of the mountains are quite different. Hindered by the Tibetan Plateau and the Tianshan Mountains, the wind speed at the southern slope is smaller than that at the northern slope, especially in summer. Compared with the northern basin (Junggar Basin), the southern basin (Tarim Basin) is more closed (judged by the relative elevation difference), and the surrounding mountain ranges are generally higher than 4000 m asl. The transport time and distance of vapor to the study region is greatly influenced by the air regime and topography. Although the total column vapor flux at the two slopes, generally, is of similar magnitude (Figures 5e and 5f), the vapor flux at the lower air column from surface to 700 hPa shows different spatial patterns (Figures 5g and 5h). In winter (Figure 5g), the vapor flux at the northern and southern slopes is all small, and the precipitation is also generally limited; in summer (Figure 5h), the vapor flux at the northern slope is obviously larger than the southern slope. It is clear that most water vapor concentrates at the bottom of the air column near the surface. In the southern basin, the mean elevation is approximately 1000 m asl, and the surrounding mountain ranges are mainly higher than 4000 m asl (even up to ~8600 m asl at some peaks). In contrast, the northern basin is relatively open, and many mountain passes with lower altitudes are located at the western side (the upwind direction), resulting in a relatively fluent transport path for westerly winds.

Westerlies are widely accepted as the dominant moisture transport drivers in arid central Asia, in almost all the studies of meteorology [e.g., *Dai et al.*, 2007; *Huang et al.*, 2015] and isotope hydrology [e.g., *Tian et al.*, 2007; *Liu et al.*, 2009; *Feng et al.*, 2013]. Across High Asia (including the Tibetan Plateau and neighboring mountains), a seasonal trend of enriched stable isotopes in summer and depleted values in winter is considered as a typical feature of westerly dominance, as opposed to Indian monsoon dominance [*Yao et al.*, 2013]. As observed in the current network in arid central Asia, the seasonal characteristics are similar for different stations, and isotopes are always enriched in summer and depleted in winter leaving no doubt that the westerlies are dominant. It has been observed that the high latitudes have depleted heavy isotope values in both vapor and precipitation [*Bowen and Revenaugh*, 2003; *Yoshimura et al.*, 2011], and the westerly moisture delivered via different latitude paths may lead to variation in precipitation isotope ratios [*Liu et al.*, 2015].

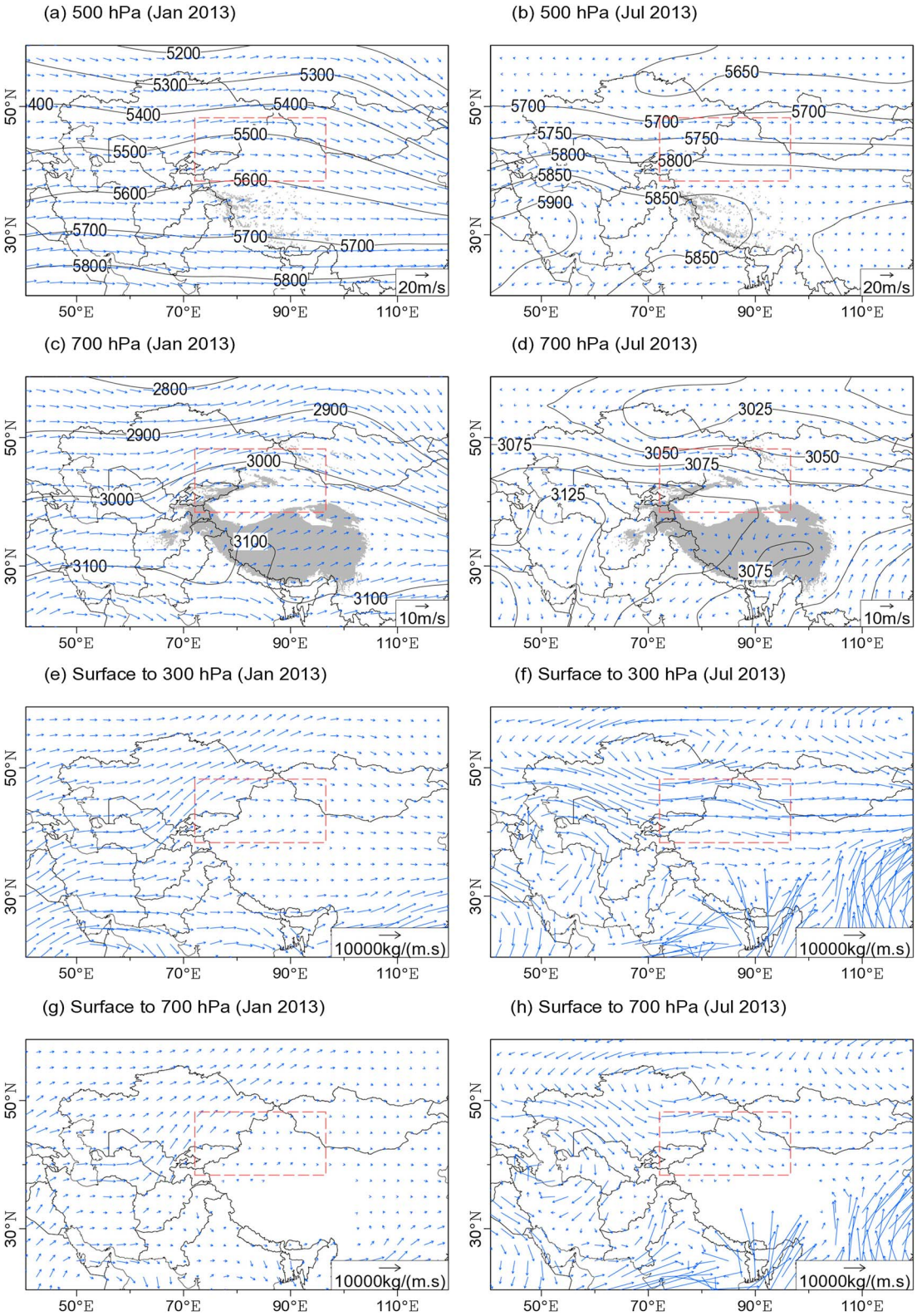

Figure 5. (a–d) Geopotential height in geopotential meters and wind field in m/s at 500 hPa and 700 hPa and (e–h) water vapor flux in kg/(m s) from surface to 300 hPa and 700 hPa for January and July 2013 based on NCEP/NCAR Reanalysis 1. Gray shades in Figures 5a and 5b and 5c and 5d indicate elevation higher than 5500 m asl (corresponds to ~500 hPa) and 3000 m asl (corresponds to ~700 hPa), respectively. Red dashed frames for each subfigure mark the study region.

In this study, this influence of northward and southward shifts in the westerly circulation can also be detected, where the northern stations have trajectories more frequently across the high latitudes and precipitation from these events usually has relatively depleted isotopic composition (as seen in Figure 4b).

The orographic controls on precipitation water isotope have been presented in many studies [e.g., *Liebminger et al*., 2006; *Liotta et al*., 2006; *Guan et al*., 2009]. As shown in Figure 5, based on reanalysis database, the moisture advection is greatly controlled by the mountain ranges surrounding the basin, and the westerly vapor flux is very different for the two sides of the Tianshan Mountains. In summer months, the moisture transport via the lower atmosphere is much weaker at the southern slope than that at the northern slope (Figures 5f and 5h), and the mountain ranges hinder the movement of westerly moisture to the arid leeward basin. Compared with the southern slope stations, the northern slope stations usually have lower air temperature, larger precipitation amount, and more frequent precipitation events. In this observation network across the Tianshan Mountains, the influence of below-cloud evaporation is more significant at the southern slope sites than the northern sites [*Wang et al*., 2016c].

3.2. Synoptic Controls on Precipitation Isotopes

Precipitation isotope ratios are usually impacted by many factors including air temperature and precipitation amount, and it is necessary to normalize for these by comparing the isotopic characteristics of events with similar meteorological conditions. Here we focus on precipitation occurring during summer (June, July, and August) of 2013 under relatively warm and wet conditions. Small rainfall samples commonly experience evaporation in the atmosphere as they fall below the cloud [*Dansgaard*, 1964; *Salamalikis et al*., 2016; *Wang et al*., 2016c]; thus, only 48 samples at 19 stations representing heavy precipitation of $\geq$10 mm are considered. Among these stations, there are eight stations with heavy rain samples occurring on no less than three occasions in the summer of 2013, i.e., Jinghe (N2), Urumqi (N6), and Qitai (N7) on the northern slope; Wuqia (M1), Akqi (M2), Bayanbulak (M3), and Balguntay (M4) in the mountains; and Aksu (S1) on the southern slope (Table 1a). The heavy rain events were more frequent on the northern slope and the mountains than those on the southern slope. From the 10 sampling stations on the southern slope, there is only one station (Aksu) with $\geq$3 heavy rain events. For the three samples in Aksu, the value of δD for one event (14–15 June 2013) was $-$0.1‰, although the rain amount was not very small (17.0 mm).

Analyzing the isotopic composition at these eight stations under different synoptic systems (Table 1b), the precipitation amount weighted values of δD are $-$60.3‰, $-$29.2‰, and $-$23.6‰, respectively, for central Asian vortex, central Asian short-wave trough, and northern frontal zone trough. Similar patterns can be found in δ^{18}O. The events influenced by the central Asian vortex have significantly more depleted D and ^{18}O values. For example, in Urumqi, the value of δD under central Asian vortex was $-$89.9‰ (19–20 June 2013), and δD under central Asian short-wave trough and northern frontal zone trough ranged from $-$50.5‰ (24 June 2013) to $-$18.1‰ (30–31 August 2013). A similar pattern was seen in most stations, although the influence of meteorological factors (including air temperature, precipitation amount, and relative humidity) still plays a role to some degree.

The relationship between synoptic systems and precipitation isotopes has been investigated in regions with multiple moisture sources [e.g., *Guan et al*., 2013; *Crawford et al*., 2013], and the variability in trajectories controlled by synoptic systems can usually be related to precipitation isotopes. However, in arid central Asia, the westerly transport can be detected for all the seasons. That is, although synoptic conditions vary, the westerly is always dominant, which is in contrast to previous studies mentioned above. Although the relationship between central Asian vortex and precipitation process in the study region was analyzed in some meteorological studies [e.g., *Zhang et al*., 2012; *Yang et al*., 2015], the relationship between synoptic system and isotopic composition has not been reported before.

In our network, the central Asian vortex usually presents a depleted isotopic composition with a lower D-excess. This synoptic type is characterized by strong convection resulting in continuous storms [*Zhang and Deng*, 1987]. Convection has been shown to result in a similar isotopic signature on the southern Tibetan Plateau [*Gao et al*., 2013]; however, over the southern Tibetan Plateau moisture is primarily derived from the Indian monsoon and depletion results from orographic effects and rainout. In this region, we may be seeing a contribution of isotopically depleted northern vapor (Figure 4b) as well as local recycled moisture, with high rainfall intensity reducing the opportunity for raindrop evaporation or exchange. As seen in

Table 1a. Meteorological Information (*T*—Air Temperature, *P*—Precipitation Amount, *h*—Relative Humidity, and Synoptic System) and Isotopic Ratios of Heavy Rains ($P \geq 10$ mm per Event) at Stations With ≥3 Samples Around the Tianshan Mountains During Summer 2013

Station	Date	*T* (°C)	*P* (mm)	*h* (%)	δD (‰)	δ^{18}O (‰)	D-Excess (‰)	System[a]
Jinghe (N2)	6–7 Jun	16.2	10.2	78	−22.9	−4.1	10.3	ST
	18–19 Jun	15.0	10.5	83	−38.0	−5.5	5.9	V
	22–23 Jul	18.9	31.1	85	−35.6	−5.9	11.3	V
Urumqi (N6)	19–20 Jun	12.8	16.6	96	−89.9	−13.3	16.4	V
	24 Jun	17.5	10.1	90	−50.5	−7.5	9.7	ST
	15–16 Jul	16.5	11.9	96	−42.3	−7.3	15.8	NT
	30–31 Aug	10.3	14.1	95	−18.1	−5.2	23.7	NT
Qitai (N7)	20 Jun	12.7	15.4	92	−80.3	−12.0	15.8	V
	15–16 Jul	16.1	11.4	90	−55.9	−9.5	20.5	NT
	18 Aug	14.7	18.9	85	−50.0	−8.3	16.2	ST
	26 Aug	15.7	12.4	87	−48.9	−9.4	26.4	ST
	30–31 Aug	10.4	18.0	88	−22.4	−6.3	27.7	NT
Wuqia (M1)	16 Jun	8.3	17.8	88	−13.1	−4.2	20.8	ST
	10–11 Jul	9.8	19.3	89	−32.5	−6.6	20.2	ST
	19 Aug	12.5	17.2	89	−20.5	−4.3	14.3	ST
Akqi (M2)	17–18 Jun	10.3	10.0	88	−25.4	−4.7	12.4	NT
	12–13 Aug	12.1	38.8	88	−15.1	−2.2	2.7	NT
	15–16 Aug	12.1	16.5	86	−13.6	−3.8	16.5	NT
	19–20 Aug	13.0	15.2	88	−13.7	−3.7	16.1	ST
	20–21 Aug	12.2	15.3	88	−18.6	−2.4	0.4	ST
Bayanbulak (M3)	19 Jun	1.8	15.4	90	−140.9	−19.6	15.5	V
	13 Aug	7.8	13.0	89	−49.8	−8.7	19.9	NT
	26–27 Aug	9.4	26.0	65	−55.7	−9.5	20.4	ST
Balguntay (M4)	15–16 Jun	10.8	10.0	91	−44.6	−7.7	16.7	ST
	19 Jun	12.4	14.5	90	−62.6	−9.2	10.7	V
	2 Jul	12.7	22.0	90	−7.3	−1.5	5.1	NT
	22–23 Jul	11.2	18.4	94	12.9	0.1	12.4	V
	17–18 Aug	11.2	11.9	87	−55.5	−9.1	17.5	V
Aksu (S1)	14–15 Jun	13.9	17.0	83	−0.1	−2.4	18.9	ST
	16–17 Jun	14.1	31.8	89	−17.9	−5.2	24.0	ST
	18 Jun	13.5	31.3	88	−71.0	−10.0	8.6	V

[a]V = central Asian vortex, ST = central Asian short-wave trough, and NT = northern frontal zone trough.

Tables 1a and 1b, the precipitation amount from this synoptic type is not the highest, so the heavy isotope depletion cannot be attributed to the amount effect. As presented in *Liu et al*. [2015], the westerly moisture path variability may influence the isotopic fractionation of precipitation in arid central Asia. In addition, the convective processes of the vortex also mean that locally recycled vapor may contribute more to precipitating vapor in atmosphere, and local moisture is usually isotopically depleted. Although the regional background is arid, the recycled moisture contributed from oases cannot be ignored [*Wang et al*., 2016b; *Li et al*., 2016a] and the lakes of Eastern Kazakhstan may also contribute.

3.3. Precipitation Isotopes and Lagrangian Diagnosed Moisture Paths

The Lagrangian approach has been widely applied to diagnose air mass transport as well as to identify moisture sources, but the setting of constant backward duration and starting height can contribute to some uncertainty. In addition, traditional approaches do not consider meteorological variables which may lead to the erroneous identification of a moisture source in instances where the moisture had rained out prior to the

Table 1b. Precipitation Amount Weighted Averages (With Arithmetic Averages ± Standard Deviation in Brackets) for Each Synoptic System

System[a]	*n*	T_{avg} (°C)	P_{avg} (mm)	h_{avg} (%)	δD_{avg} (‰)	$\delta^{18}O_{avg}$ (‰)	D-Excess$_{avg}$ (‰)
V	9	12.9 (12.2 ± 4.5)	165.1[b] (18.3 ± 7.7)	89 (89 ± 4)	−60.3 (−62.3 ± 42.3)	−9.1 (−9.4 ± 5.5)	12.3 (12.7 ± 3.9)
ST	13	12.6 (12.9 ± 2.8)	221.2[b] (17.0 ± 6.3)	85 (85 ± 7)	−29.2 (−29.9 ± 18.1)	−5.8 (−5.8 ± 2.5)	17.5 (16.5 ± 6.8)
NT	9	12.0 (12.0 ± 2.8)	155.7[b] (17.3 ± 8.9)	89 (90 ± 3)	−23.6 (−27.8 ± 17.3)	−4.7 (−5.5 ± 2.7)	13.7 (16.0 ± 8.2)

[a]V = central Asian vortex, ST = central Asian short-wave trough, and NT = northern frontal zone trough.
[b]Total precipitation.

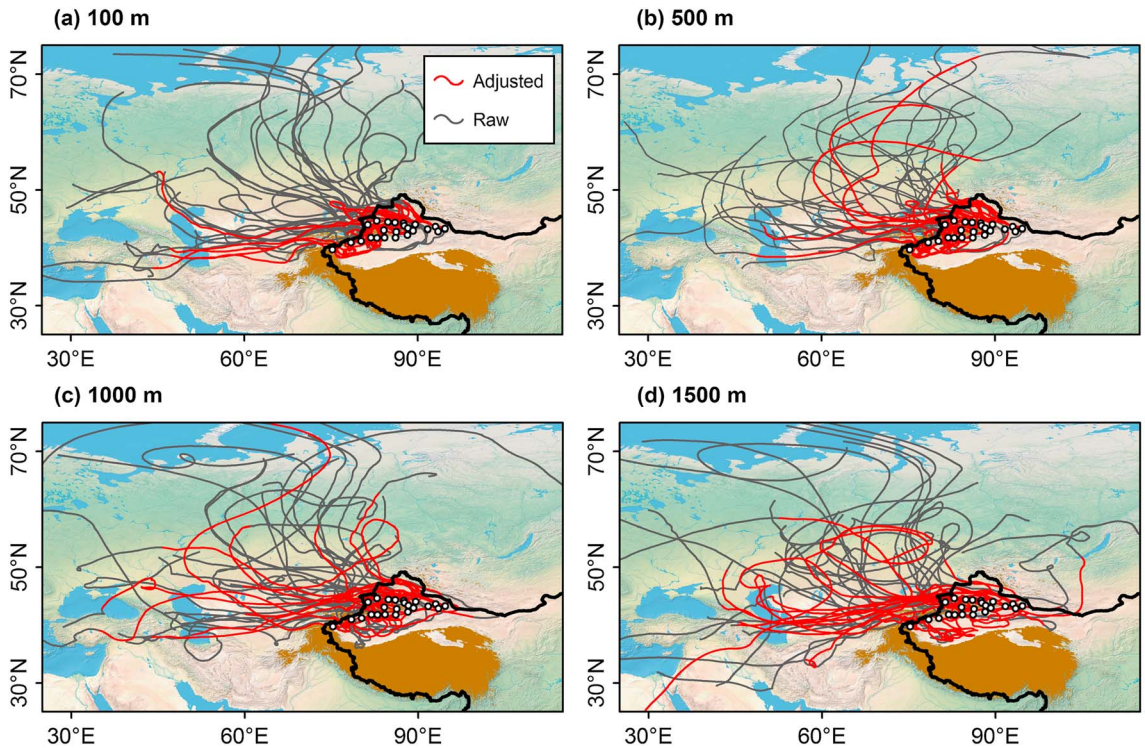

Figure 6. Spatial distribution of raw and adjusted trajectories to target heights (100 m, 500 m, 1000 m, and 1500 m above ground level) of sampling stations for each heavy precipitation event around the Tianshan Mountains in summer 2013. The specific humidity-adjusted trajectories are marked as red curves, and the raw trajectories are marked as grey curves (and overlying red curves). The sampling stations in the observation network are marked as empty circles. The black curve denotes the national boundary of China, and the brown shadow denotes the Tibetan Plateau with elevation >3000 m above sea level. The satellite-derived land cover is acquired from Natural Earth (http://www.naturalearthdata.com). A zoomed map focused in the Tianshan Mountains is shown in supporting information Figure S1.

air mass arriving at the sampling site. A Lagrangian diagnostic adjusted using specific humidity [e.g., *Sodemann et al*., 2008; *Crawford et al*., 2013] may improve backward trajectory to some degree; however, this has not been previously applied in an arid setting. Using the method described in section 2.4, the backward trajectory with a selected constant duration can be adjusted according to the variation of specific humidity along the air mass path, and the trajectory length can be reduced to the location where the specific humidity is less than a specified threshold.

Figure 6 shows the differences between raw and specific humidity-adjusted trajectories for the heavy precipitation events in the summer of 2013 (zoomed-in maps focused on the sampling sites are provided in Figure S1 in the supporting information). It is clear that the adjusted trajectories are shorter than those of the raw result. The marine moisture source in central Asia is usually considered as the Atlantic Ocean, which is very clear for the upper atmosphere [*Hu*, 2004]. However, the adjusted moisture paths are generally similar and originate mostly from central Asia. The huge mountain ranges to the south hinder most southern moisture (i.e., the Indian Monsoon via the Arabian Sea and the Bay of Bengal) to the study region. Classifying into terrestrial and ocean sources by visual inspection of the back trajectories, the terrestrial source is more meaningful, and the direct moisture sourced from oceans is very limited. From the spatial distribution of the adjusted back trajectories it is evident that the moisture leading to precipitation at the sampling sites is more likely to have been sourced over Europe and central Asia, rather than from the Atlantic Ocean.

Using the specific humidity-adjusted Lagrangian method, we can investigate the influence of moisture paths on precipitation isotopes for the northern and southern slopes (Figures 7 and S2). Although different starting heights are presented, the westerly fetch is always dominant. The backward trajectories at the northern slope sites rarely pass over the Tarim Basin in the south, especially for back trajectories with starting heights of less than 1000 m above ground level. Generally, the precipitation at the northern slope sites is more likely to be depleted, and precipitation with δ^{18}O of -5‰, or higher, is usually seen at the southern slope stations. The

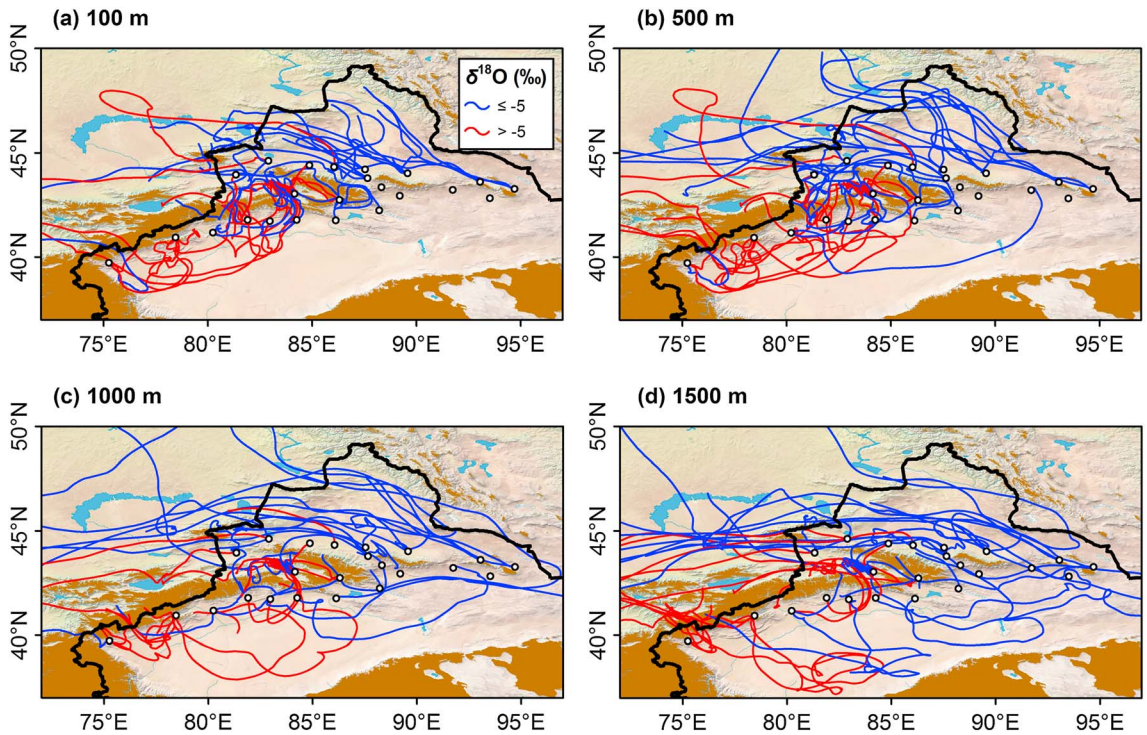

Figure 7. Spatial distribution of adjusted trajectories to target heights (100 m, 500 m, 1000 m, and 1500 m above ground level) of sampling stations for each heavy precipitation event around the Tianshan Mountains in summer 2013. The measured isotope ratios in precipitation at target stations are marked as different colors. The sampling stations in the observation network are marked as empty circles. The black curve denotes the national boundary of China, and the brown shadow denotes the Tibetan Plateau with elevation >3000 m above sea level. The satellite-derived land cover is acquired from Natural Earth (http://www.naturalearthdata.com). A map showing full trajectories is shown in supporting information Figure S2.

northern and southern stations differ in isotopic signature as well as moisture transport trajectory. The trajectories at the northern part of central Asia (more depleted) are more likely to influence the northern slope sites, as the Tianshan Mountains hinders their passage to the southern slope sites. The different starting heights do influence the results, but the main trajectory pattern is still stable.

In some publications on isotopic modeling of falling rain drops [e.g., *Salamalikis et al.*, 2016], the 850 hPa heights (~1500 m asl) were approximately considered as cloud-based heights or precipitating heights. However, the assumption is not always valid in our network, because many mountainous sites in the Tianshan Mountains are higher than 1500 m. The lifting condensation level has been considered to be an effective approach to estimate cloud-based height [e.g., *Fletcher and Bretherton*, 2010; *Wang et al.*, 2016c]. *Wang et al.* [2016c] estimated the cloud-based heights for each precipitation event in the Tianshan Mountains and calculated an average height in summer of 657 ± 454 m; the proportions with estimated heights ≤100 m, 100–500 m, 500–1000 m, 1000–1500 m, and >1500 m were 2.1%, 42.3%, 37.9%, 10.6%, and 7.1%, respectively. The altitudes of 100 m, 500 m, 1000 m, and 1500 m were selected in the current study and were included for completeness of the analysis. As shown in Figures 5f and 5h, although a large vapor flux results from higher elevations (higher than 700 hPa or ~3000 m asl) in summer, the upper air moisture is not likely to lead to precipitation in arid central Asia, which has been evidenced by many meteorological studies [e.g., *Li and Zhang*, 2003; *Zhao et al.*, 2010; *Yang et al.*, 2013].

The results from a sensitivity analysis on the threshold of specific humidity are presented in Figures 8 and S3. The starting heights, of the back trajectories, were set at 500 m above ground level, and four threshold values (from 0.1 g/kg to 0.4 g/kg with step width of 0.1 g/kg) of specific humidity were applied in the adjusting method. Generally, the adjusted trajectories were not very sensitive to the selection of the threshold value. For threshold values of 0.2 g/kg and less, little difference in the length of the back trajectory was seen (Figures S3a and S3b), indicating that the same moisture sources lead to precipitation at the measurement sites. As the threshold value was increased, the back trajectories indicated that the predominant moisture

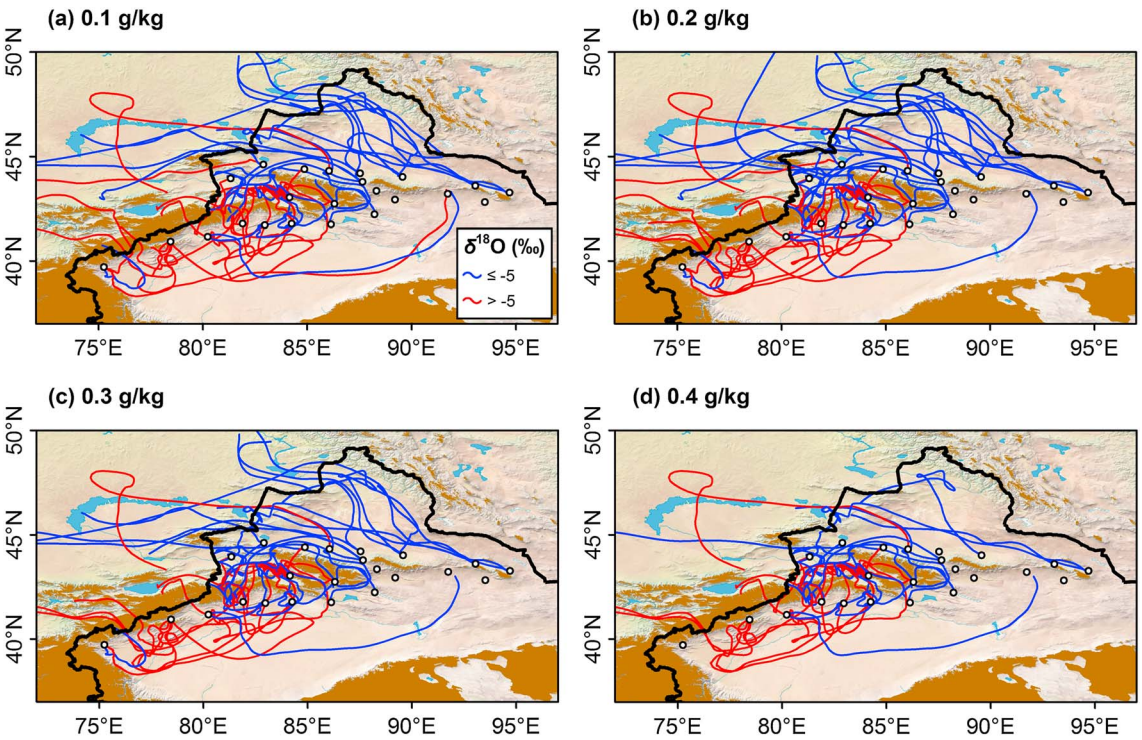

Figure 8. Spatial distribution of adjusted trajectories to sampling stations for each heavy precipitation event around the Tianshan Mountains using different specific humidity thresholds (0.1 g/kg, 0.2 g/kg, 0.3 k/kg, and 0.4 g/kg) in summer 2013. The measured isotope ratios in precipitation are marked as different colors. The target height is set as 500 m above ground level. The sampling stations in the observation network are marked as empty circles. The black curve denotes the national boundary of China, and the brown shadow denotes the Tibetan Plateau with elevation >3000 m above sea level. The satellite-derived land cover is acquired from Natural Earth (http://www.naturalearthdata.com). A map showing full trajectories is shown in supporting information Figure S3.

sources were closer to the measurement sites. This is an expected result as fewer vapor sources are available in the arid region farther from the sites.

Generally, the trajectory results using different parameters remain similar, and the default specific humidity parameter used in previous studies [*Sodemann et al.*, 2008; *Crawford et al.*, 2013] is meaningful for the study domain. The adjusted approach is not very sensitive to the specific humidity thresholds. It should be noticed that the trajectories and the detected potential moisture sources are related to the starting height, because vapor transport in the upper atmosphere is more fluent than that in the lower atmosphere. The adjusted Lagrangian approach based on specific humidity along the back trajectory is valid for arid central Asia, and the improved result is meaningful even under an arid condition.

3.4. Isotopic Evolution of Rainfall Along the Trajectory

The evolution of rain events across this large region may also give us some insight into rainout, so we focus on the isotopic compositions at all the sampling sites for two large precipitation events around 18–20 June and 25–27 August 2013 (Figures 9 and 10), where some heavy rains were observed across the region (Tables 1a and 1b). It is clear that the rain belts move from west to east for both events, although the two processes are controlled by different synoptic systems (central Asian vortex and central Asian short-wave trough) which result in markedly different trajectories. As the rain belt moves eastward, the isotopic composition of precipitation becomes more depleted in the heavy isotopes (Figure 9). For the northern slope stations, the depleting trend in isotopes is obvious, although Jinghe (N2) is usually isotopically more enriched than Yining (N1) presumably because the mountain range between the two sites means that they do not generally lie along the same trajectory. From Jinghe (N2) to Qitai (N7) the moisture path is fluent, and precipitation isotopes show clear depletion along the vapor transport trajectory. For the southern slope, with smaller precipitation amounts, whilst the time sequence for precipitation events in these stations coincides with the passage of the synoptic system, significant below-cloud process (as discussed in *Wang et al.* [2016c]) and complex trajectory paths, particularly for the central Asian vortex (Figure 10a), may impact on

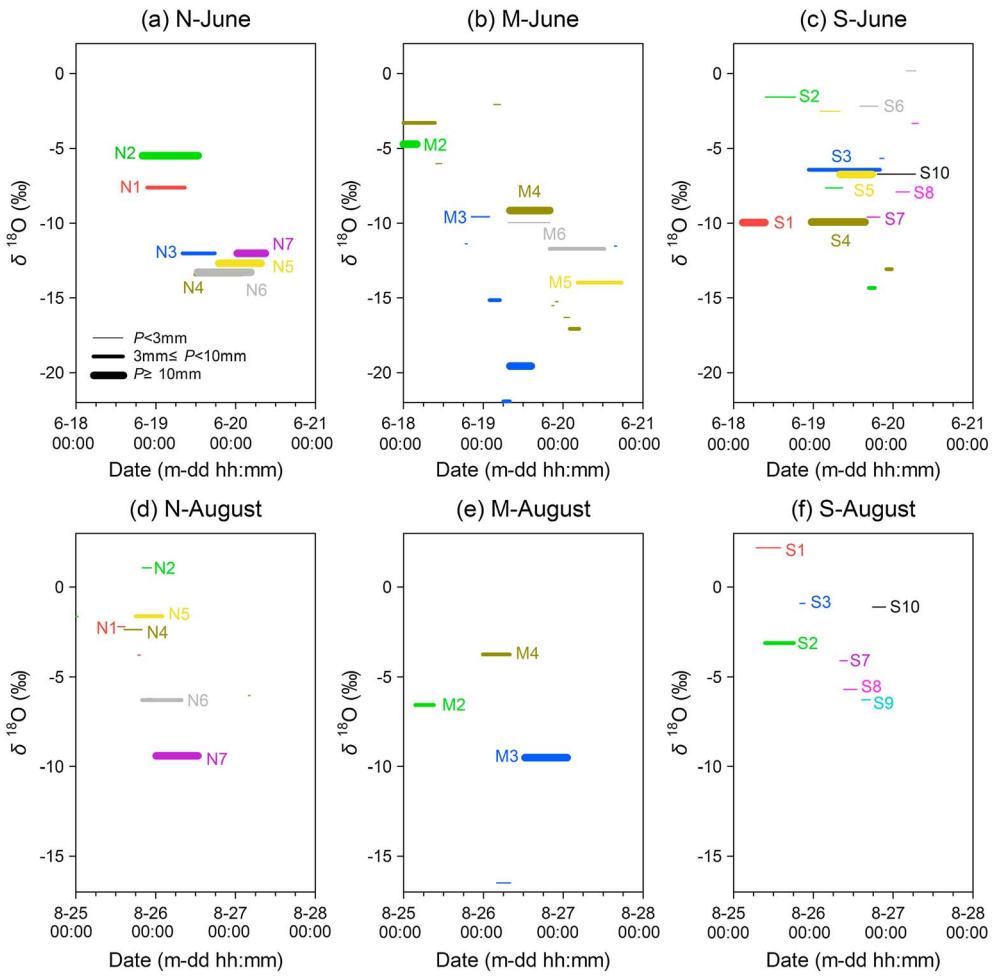

Figure 9. Variation of δ^{18}O in precipitation at all sampling sites around the Tianshan Mountains in (a–c) 18–20 June 2013 and (d–f) 25–27 August 2013 around the Tianshan Mountains. In each subfigure, the different colors denote the station name, and the station codes are labeled, respectively. One color corresponds to a single station and therefore that multiple bars of the same color represent multiple samples from one site. The length of the bar represents the time where the rain fell. The thickness of line denotes the precipitation amount for each event, i.e., $P < 3$ mm, 3 mm $\leq P < 10$ mm, and $P \geq 10$ mm.

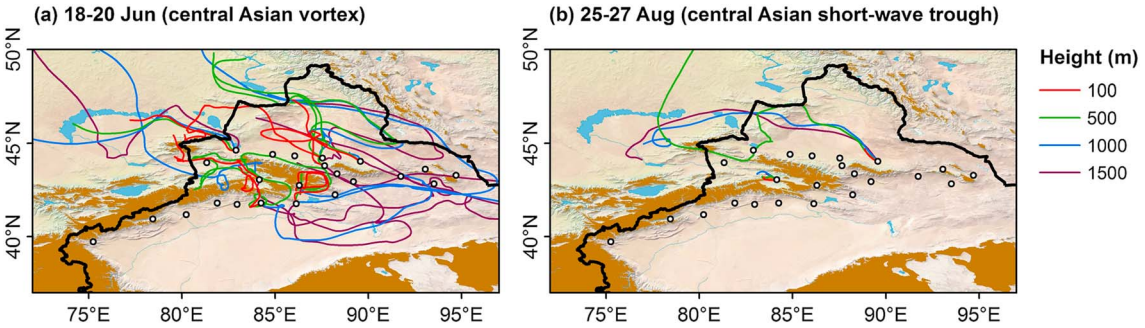

Figure 10. Spatial distribution of adjusted trajectories to target heights (100 m, 500 m, 1000 m, and 1500 m above ground level) of sampling stations for each heavy precipitation event around the Tianshan Mountains in (a) 18–20 June (central Asian vortex) and (b) 25–27 August (central Asian short-wave trough) 2013. The target heights for each station are marked as different colors. The sampling stations in the observation network are marked as empty circles. The black curve denotes the national boundary of China, and the brown shadow denotes the Tibetan Plateau with elevation >3000 m above sea level. The satellite-derived land cover is acquired from Natural Earth (http://www.naturalearthdata.com).

the rainfall isotopic ratios along the trajectory. The rain amounts are very small at the moisture downstream areas like Turpan (S8, 0.5 mm and 2.6 mm in Figures 9c and 9f), Shisanjianfang (S9, 0 mm and 0.7 mm), and Hami (S10, 2.2 mm and 0.5 mm). The different isotopic characteristics for the two sides of the Tianshan Mountains indicate that the local influence may be more significant at the southern slope stations. For the mountains, the sites are sufficiently distant from each other and the elevations and aspects so variable that evolution of rainfall between sites is not seen. However, Figure 9b shows depletion between consecutive samples collected at each site for the June event which can be interpreted as a rainout effect.

For a small region, the altitude effect (negative correlation between isotopic ratio and elevation) usually exists for the mountains. However, for such a large region with length of ~1700 km from west to east, the altitude effect is not always the most significant. The rainout pathway from west to east, the large variation in latitude, and the temperature variation with elevation are all contributors to what may be perceived as an altitude effect. In our previous study [*Wang et al*., 2016a], the altitude effect is only seen to be significant in summer, and the different climate conditions of the mountains near the northern slope and southern slope make it hard to relate variability to altitude alone.

4. Conclusion

Compared with coastal and island sites with potential oceanic evaporative sources from many or all directions, the contribution of terrestrial evapotranspiration to the local precipitation is much greater in arid and semiarid regions of central Asia, and the dominant upwind direction (i.e., westerlies) is more coherent. Based on an observation network of isotopes in precipitation around the Tianshan Mountains in central Asia, the moisture sources and synoptic effect on precipitation isotope composition were investigated. A Lagrangian diagnostic adjusted using specific humidity, which has not been previously applied in an arid setting, was applied to identify the moisture sources for each precipitation event. The adjusted trajectories were usually shorter than the raw ones, which may lead to a more meaningful result. Previously, the Atlantic Ocean has been considered as the primary marine moisture source in central Asia. However, most adjusted trajectories cannot reach the Atlantic Ocean, and the terrestrial moisture evaporated from Europe and central Asia may instead be the main moisture sources. The sensitivity analysis for target height and specific humidity threshold indicates that this improved approach is valid in an arid climate. Among the main synoptic systems in the study region, the central Asian vortex usually corresponds to the rain events with the most depleted isotopic ratios, which is considered to be related to the contribution of northerly moisture and/or locally recycled moisture with depleted isotopes. Because of the small number of significant rainfall events in such an arid climate, a longer time series would be of benefit in investigating both synoptic and rainout progresses in this region.

Acknowledgments
The research is supported by the National Natural Science Foundation of China (41161012 and 41240001), the National Basic Research Program of China (2013CBA01801), the Foundation for Young Teachers of Northwest Normal University (NWNU-LKQN-15-8), and the Desert Meteorology Research Foundation of China (Sqj2016001). The authors greatly thank the Xinjiang Meteorological Bureau and all the meteorological stations for collecting the precipitation samples and the colleagues in the Northwest Normal University for their help in field work, laboratory analysis, and data processing. Thanks to Gaofei Wang, Fan Xiang (Meteorological Bureau of Kizilsu Kirgiz Autonomous Prefecture), Junqiang Yao (Institute of Desert Meteorology, China Meteorological Administration, Urumqi), and Xiaoyan Huang (Institute of Arid Meteorology, China Meteorological Administration, Lanzhou) for meteorological analyzing. Thanks also to Stephen Good (Oregon State University) and two anonymous reviewers for their constructive suggestions. The data in this paper are available from Shengjie Wang (geowang@126.com) upon request.

References

Bailey, H. L., D. S. Kaufman, A. C. G. Henderson, and M. J. Leng (2015), Synoptic scale controls on the δ^{18}O in precipitation across Beringia, *Geophys. Res. Lett.*, *42*, 4608–4616, doi:10.1002/2015GL063983.

Bershaw, J., S. M. Penny, and C. N. Garzione (2012), Stable isotopes of modern water across the Himalaya and eastern Tibetan Plateau: Implications for estimates of paleoelevation and paleoclimate, *J. Geophys. Res.*, *117*, D02110, doi:10.1029/2011JD016132.

Bosilovich, M. G., and S. D. Schubert (2002), Water vapor tracers as diagnostics of the regional hydrologic cycle, *J. Hydrometeorol.*, *3*, 149–165, doi:10.1175/1525-7541(2002)003<0149:WVTADO>2.0.CO;2.

Bowen, G. J., and J. Revenaugh (2003), Interpolating the isotopic composition of modern meteoric precipitation, *Water Resour. Res.*, *39*, 1299, doi:10.1029/2003WR002086.

Crawford, J., C. E. Hughes, and S. D. Parkes (2013), Is the isotopic composition of event based precipitation driven by moisture source or synoptic scale weather in the Sydney Basin, Australia?, *J. Hydrol.*, *507*, 213–226, doi:10.1016/j.jhydrol.2013.10.031.

Crawford, J., S. E. Hollins, K. T. Meredith, and C. E. Hughes (2017), Precipitation stable isotope variability and subcloud evaporation processes in a semi-arid region, *Hydrol. Processes*, *31*, 20–34, doi:10.1002/hyp.10885.

Dai, X., W. Li, Z. Ma, and P. Wang (2007), Water-vapor source shift of Xinjiang region during the recent twenty years, *Prog. Nat. Sci.*, *17*, 569–575, doi:10.1080/10020070708541037.

Dansgaard, W. (1964), Stable isotopes in precipitation, *Tellus*, *16*, 436–468, doi:10.1111/j.2153-3490.1964.tb00181.x.

Draxler, R. R., and G. D. Hess (1998), An overview of HYSPLIT_4 modelling system for trajectories, dispersion and deposition, *Aust. Meteorol. Mag.*, *47*, 295–308.

Draxler, R. R., and G. D. Rolph (2016), HYSPLIT (HYbrid Single-Particle Lagrangian Integrated Trajectory) Model, NOAA Air Resources Laboratory. [Available at http://www.arl.noaa.gov/HYSPLIT.php.]

Feng, F., Z. Li, M. Zhang, S. Jin, and Z. Dong (2013), Deuterium and oxygen 18 in precipitation and atmospheric moisture in the upper Urumqi River Basin, eastern Tianshan Mountains, *Environ. Earth Sci.*, *68*, 1199–1209, doi:10.1007/s12665-012-1820-y.

Fletcher, J. K., and C. S. Bretherton (2010), Evaluating boundary layer-based mass flux closures using cloud-resolving model simulations of deep convection, *J. Atmos. Sci.*, *67*, 2212–2225, doi:10.1175/2010JAS3328.1.

Gao, J., V. Masson-Delmotte, C. Risi, Y. He, and T. Yao (2013), What controls precipitation δ^{18}O in the southern Tibetan Plateau at seasonal and intra-seasonal scales? A case study at Lhasa and Nyalam, *Tellus B*, *65*, 21,043, doi:10.3402/tellusb.v65i0.21043.

Gat, J. R. (2000), Atmospheric water balance—The isotopic perspective, *Hydrol. Processes*, *14*, 1357–1369, doi:10.1002/1099-1085(20000615)14:8<1357::AID-HYP986>3.0.CO;2-7.

Gat, J. R., and I. Carmi (1970), Evolution of the isotopic composition of the atmospheric water in the Mediterranean Sea area, *J. Geophys. Res.*, *75*, 3039–3048, doi:10.1029/JC075i015p03039.

Gimeno, L., A. Stohl, R. M. Trigo, F. Dominguez, K. Yoshimura, L. Yu, A. Drumond, A. M. Durán-Quesada, and R. Nieto (2012), Oceanic and terrestrial sources of continental precipitation, *Rev. Geophys.*, *50*, RG4003, doi:10.1029/2012RG000389.

Gimeno, L., R. Nieto, A. Drumond, R. Castillo, and R. Trigo (2013), Influence of the intensification of the major oceanic moisture sources on continental precipitation, *Geophys. Res. Lett.*, *40*, 1443–1450, doi:10.1002/grl.50338.

Good, S. P., D. V. Mallia, J. C. Lin, and G. J. Bowen (2014), Stable isotope analysis of precipitation samples obtained via crowdsourcing reveals the spatiotemporal evolution of Superstorm Sandy, *PLoS One*, *9*, e91117, doi:10.1371/journal.pone.0091117.

Good, S. P., D. Noone, N. Kurita, M. Benetti, and G. J. Bowen (2015), D/H isotope ratios in the global hydrologic cycle, *Geophys. Res. Lett.*, *42*, 5042–5050, doi:10.1002/2015GL064117.

Guan, H., C. T. Simmons, and A. J. Love (2009), Orographic controls on rain water isotope distribution in the Mount Lofty Ranges of South Australia, *J. Hydrol.*, *374*, 255–264, doi:10.1016/j.jhydrol.2009.06.018.

Guan, H., X. Zhang, G. Skrzypek, Z. Sun, and X. Xu (2013), Deuterium excess variations of rainfall events in a coastal area of South Australia and its relationship with synoptic weather systems and atmospheric moisture sources, *J. Geophys. Res. Atmos.*, *118*, 1123–1138, doi:10.1002/jgrd.50137.

Hijmans, R. J., S. E. Cameron, J. L. Parra, P. G. Jones, and A. Jarvis (2005), Very high resolution interpolated climate surfaces for global land areas, *Int. J. Climatol.*, *25*, 1965–1978, doi:10.1002/joc.1276.

Hu, R. (2004), *Physical Geography of the Tianshan Mountains in China* [in Chinese], China Environmental Science Press, Beijing.

Huang, W., J. Chen, X. Zhang, S. Feng, and F. Chen (2015), Definition of the core zone of the "westerlies-dominated climatic regime", and its controlling factors during the instrumental period, *Sci. China Earth Sci.*, *58*, 676–684, doi:10.1007/s11430-015-5057-y.

Jouzel, J., G. Delaygue, A. Landais, V. Masson-Delmotte, C. Risi, and F. Vimeux (2013), Water isotopes as tools to document oceanic sources of precipitation, *Water Resour. Res.*, *49*, 7469–7486, doi:10.1002/2013WR013508.

Kalnay, E., et al. (1996), The NCEP/NCAR 40-year reanalysis project, *Bull. Am. Meteorol. Soc.*, *77*, 437–471, doi:10.1175/1520-0477(1996)077<0437:TNYRP>2.0.CO;2.

Kistler, R., et al. (2001), The NCEP-NCAR 50-year reanalysis: Monthly means CD-ROM and documentation, *Bull. Am. Meteorol. Soc.*, *82*, 247–268, doi:10.1175/1520-0477(2001)082<0247:TNNYRM>2.3.CO;2.

Kleist, D. T., D. F. Parrish, J. C. Derber, R. Treadon, W.-S. Wu, and S. Lord (2009), Introduction of the GSI into the NCEP Global Data Assimilation System, *Weather Forecasting*, *24*, 1691–1705, doi:10.1175/2009WAF2222201.1.

Lavers, D. A., F. M. Ralph, D. E. Waliser, A. Gershunov, and M. D. Dettinger (2015), Climate change intensification of horizontal water vapor transport in CMIP5, *Geophys. Res. Lett.*, *42*, 5617–5625, doi:10.1002/2015GL064672.

Levin, N. E., E. J. Zipser, and T. E. Cerling (2009), Isotopic composition of waters from Ethiopia and Kenya: Insights into moisture sources for eastern Africa, *J. Geophys. Res.*, *114*, D23306, doi:10.1029/2009JD012166.

Li, X., and G. Zhang (2003), Research on precipitable water and precipitation conversion efficiency around Tianshan Mountain Area [in Chinese with English abstract], *J. Desert Res.*, *23*, 509–513.

Li, Z., Y. Gao, Y. Wang, Y. Pan, J. Li, A. Chen, T. Wang, C. Han, Y. Song, and W. H. Theakstone (2015), Can monsoon moisture arrive in the Qilian Mountains in summer?, *Quat. Int.*, *358*, 113–125, doi:10.1016/j.quaint.2014.08.046.

Li, Z., Q. Feng, Q. J. Wang, Y. Kong, A. Cheng, S. Yong, Y. Li, J. Li, and X. Guo (2016a), Contributions of local terrestrial evaporation and transpiration to precipitation using δ^{18}O and D-excess as a proxy in Shiyang inland river basin in China, *Global Planet. Change*, *146*, 140–151, doi:10.1016/j.gloplacha.2016.10.003.

Li, Z., Q. Feng, Y. Song, Q. J. Wang, J. Yang, Y. Li, J. Li, and X. Guo (2016b), Stable isotope composition of precipitation in the south and north slopes of Wushaoling Mountain, northwestern China, *Atmos. Res.*, *182*, 87–10, doi:10.1016/j.atmosres.2016.07.023.

Liebminger, A., G. Haberhauer, W. Papesch, and G. Heiss (2006), Correlation of the isotopic composition in precipitation with local conditions in alpine regions, *J. Geophys. Res.*, *111*, D05104, doi:10.1029/2005JD006258.

Liotta, M., R. Favara, and M. Valenza (2006), Isotopic composition of the precipitations in the central Mediterranean: Origin marks and orographic precipitation effects, *J. Geophys. Res.*, *111*, D05104, doi:10.1029/2005JD006818.

Liu, J., X. Song, X. Sun, G. Yuan, X. Liu, and S. Wang (2009), Isotopic composition of precipitation over Arid Northwestern China and its implications for the water vapor origin, *J. Geogr. Sci.*, *19*, 164–174, doi:10.1007/s11442-009-0164-3.

Liu, J., X. Song, G. Yuan, and X. Sun (2014), Stable isotopic compositions of precipitation in China, *Tellus B*, *66*, 22,567, doi:10.3402/tellusb.v66.22567.

Liu, X., Z. Rao, X. Zhang, W. Huang, J. Chen, and F. Chen (2015), Variations in the oxygen isotopic composition of precipitation in the Tianshan Mountains region and their significance for the Westerly circulation, *J. Geogr. Sci.*, *25*, 801–816, doi:10.1007/s11442-015-1203-x.

Pang, Z., Y. Kong, K. Froehlich, T. Huang, L. Yuan, Z. Li, and F. Wang (2011), Processes affecting isotopes in precipitation of an arid region, *Tellus B*, *63*, 352–359, doi:10.1111/j.1600-0889.2011.00532.x.

Salamalikis, V., A. A. Argiriou, and E. Dotsika (2015), Stable isotopic composition of atmospheric water vapor in Patras, Greece: A concentration weighted trajectory approach, *Atmos. Res.*, *152*, 93–104, doi:10.1016/j.atmosres.2014.02.021.

Salamalikis, V., A. A. Argiriou, and E. Dotsika (2016), Isotopic modeling of the sub-cloud evaporation effect in precipitation, *Sci. Total Environ.*, *544*, 1059–1072, doi:10.1016/j.scitotenv.2015.11.072.

Salati, E., A. D. Olio, E. Matsui, and J. R. Gat (1979), Recycling of water in the Amazon Basin: An isotopic study, *Water Resour. Res.*, *15*, 1250–1258, doi:10.1029/WR015i005p01250.

Shi, Y., Z. Sun, and Q. Yang (2008), Characteristics of area precipitation in Xinjiang region with its variations [in Chinese with English abstract], *J. Appl. Meteorol. Sci.*, *19*, 326–332.

Sodemann, H., C. Schwierz, and H. Wernli (2008), Interannual variability of Greenland winter precipitation sources: Lagrangian moisture diagnostic and North Atlantic Oscillation influence, *J. Geophys. Res.*, *113*, D03107, doi:10.1029/2007JD008503.

Sorg, A., T. Bolch, M. Stoffel, O. Solomina, and M. Beniston (2012), Climate change impacts on glaciers and runoff in Tien Shan (Central Asia), *Nat. Clim. Change*, *2*, 725–731, doi:10.1038/nclimate1592.

Steen-Larsen, H. C., A. E. Sveinbjörnsdottir, T. Jonsson, F. Ritter, J.-L. Bonne, V. Masson-Delmotte, H. Sodemann, T. Blunier, D. Dahl-Jensen, and B. M. Vinther (2015), Moisture sources and synoptic to seasonal variability of North Atlantic water vapor isotopic composition, *J. Geophys. Res. Atmos.*, *120*, 5757–5774, doi:10.1002/2015JD023234.

Tian, L., T. Yao, K. MacClune, J. W. C. White, A. Schilla, B. Vaughn, R. Vachon, and K. Ichiyanagi (2007), Stable isotopic variations in west China: A consideration of moisture sources, *J. Geophys. Res.*, *112*, D10112, doi:10.1029/2006JD007718.

Trenberth, K. E. (1998), Atmospheric moisture residence times and cycling: Implications for rainfall rates and climate change, *Clim. Change*, *39*, 667–694, doi:10.1023/A:1005319109110.

Wang, S., M. Zhang, C. E. Hughes, X. Zhu, L. Dong, Z. Ren, and F. Chen (2016a), Factors controlling stable isotope composition of precipitation in arid conditions: An observation network in the Tianshan Mountains, central Asia, *Tellus B*, *68*, 26,206, doi:10.3402/tellusb.v68.26206.

Wang, S., M. Zhang, Y. Che, F. Chen, and F. Qiang (2016b), Contribution of recycled moisture to precipitation in oases of arid central Asia: A stable isotope approach, *Water Resour. Res.*, *52*, 3246–3257, doi:10.1002/2015WR018135.

Wang, S., M. Zhang, Y. Che, X. Zhu, and X. Liu (2016c), Influence of below-cloud evaporation on deuterium excess in precipitation of arid central Asia and its meteorological controls, *J. Hydrometeorol.*, *17*, 1973–1984, doi:10.1175/JHM-D-15-0203.1.

Yang, L., L. Yang, H. Tang, T. Liu, and J. Peng (2013), Characteristics of water vapor transport over Tianshan Mountainous Area from 2000 to 2011 [in Chinese with English abstract], *Desert Oasis Meteorol.*, *7*, 21–25.

Yang, L., Y. Zhang, and H. Qin (2015), Some advances and problems of Middle-Asia vortex [in Chinese with English abstract], *Desert Oasis Meteorol.*, *9*, 1–8, doi:10.3969/j.issn.1002-0799.2015.05.001.

Yao, T., V. Masson, J. Jouzel, M. Stievenard, W. Sun, and K. Jiao (1999), Relationships between δ^{18}O in precipitation and surface air temperature in the Urumqi River Basin, East Tianshan Mountains, China, *Geophys. Res. Lett.*, *26*, 3473–3476, doi:10.1029/1999GL006061.

Yao, T., et al. (2013), A review of climatic controls on δ^{18}O in precipitation over the Tibetan Plateau: Observations and simulations, *Rev. Geophys.*, *51*, 525–548, doi:10.1002/rog.20023.

Ye, H., E. J. Fetzer, S. Wong, A. Behrangi, D. Yang, and B. H. Lambrigtson (2015), Increasing atmospheric water vapor and higher daily precipitation intensity over northern Eurasia, *Geophys. Res. Lett.*, *42*, 9404–9410, doi:10.1002/2015GL066104.

Yoshimura, K., C. Frankenberg, J. Lee, M. Kanamitsu, J. Worden, and T. Röckmann (2011), Comparison of an isotopic atmospheric general circulation model with new quasi-global satellite measurements of water vapor isotopologues, *J. Geophys. Res.*, *116*, D19118, doi:10.1029/2011JD016035.

Zhang, J., and Z. Deng (1987), *Introduction to Precipitation in Xinjiang* [in Chinese], China Meteorological Press, Beijing.

Zhang, M., and S. Wang (2016), A review of precipitation isotope studies in China: Basic pattern and hydrological process, *J. Geogr. Sci.*, *26*, 921–938, doi:10.1007/s11442-016-1307-y.

Zhang, X., and J. Zhang (2006), *Xinjiang Meteorological Handbook* [in Chinese], China Meteorological Press, Beijing.

Zhang, Y., L. Yang, D. Xiaokaiti, H. Qin, Y. Li, and X. Yang (2012), The central Asian vortex activity during 1971–2010 [in Chinese with English abstract], *J. Appl. Meteorol. Sci.*, *23*, 312–321.

Zhao, L., S. An, L. Yang, Y. Ma, and G. Zhang (2010), Study on precipitable water and precipitation conversion efficiency in Urumqi during the period of 1976–2007 [in Chinese with English abstract], *Arid Zone Res.*, *27*, 433–437, doi:10.13866/j.azr.2010.03.011.